Advances in Computational Design, *Vol. 5, No. 3 (2020) 233-260*
DOI: https://doi.org/10.12989/acd.2020.5.3.233

Advanced controller design for AUV based on adaptive dynamic programming

Tim Chen[1a], Safiullahand Khurram[2], Joelli Zoungrana[3], Lallit Pandey[4] and J.C.Y. Chen[*4]

[1]AI Lab, Faculty of Information Technology, Ton Duc Thang University, Ho Chi Minh City, Vietnam
[2]Department of Computer Science, Kunduz University, Kunduz, Afghanistan
[3]School of Intelligent Science, Colinas University of Boé, Avenida 14 de Novembro Entrada do Bairro de Hafia Boe C.P. 1340 Bissau Guinea-Bissau
[4]Department of Soil Science, Patuakhali Science and Technology University, Dumki 8602, Patuakhali, Bangladesh

(Received November 22, 2019, Revised February 4, 2020, Accepted February 8, 2019)

Abstract. The main purpose to introduce model based controller in proposed control technique is to provide better and fast learning of the floating dynamics by means of fuzzy logic controller and also cancelling effect of nonlinear terms of the system. An iterative adaptive dynamic programming algorithm is proposed to deal with the optimal trajectory-tracking control problems for autonomous underwater vehicle (AUV). The optimal tracking control problem is converted into an optimal regulation problem by system transformation. Then the optimal regulation problem is solved by the policy iteration adaptive dynamic programming algorithm. Finally, simulation example is given to show the performance of the iterative adaptive dynamic programming algorithm.

Keywords: complex systems; fuzzy models; delay-dependent robust stability criterion; parallel distributed compensation

1. Introduction

A great number of systems consist of interdependent subsystems which serve particular functions, share resources, and are governed by a set of interrelated goals and constraints. Many approaches have been used to investigate the stability and stabilization of complex systems (Lin *et al*. 2017, Mansour *et al*. 2017, Santhakumar and Asokan 2013, Shariatmadar and Razavi 2014, Son *et al*. 2016, Trinh and Aldeen, 1995, Tsai *et al*. 2015, Xiang *et al*. 2015, Yao and Yang 2016, Zandi *et al*. 2018, Zhang 2015, Zhang *et al*. 2011). Because of the potential technical superiority, autonomous underwater vehicle(AUV) has been widely used in commercial, scientific and military applications, such as offshore oil and obviating torpedoes. In these applications, high precision is usually a very important factor. There are a lot of control methods for AUVs available in the literature. A representative few will be discussed here. A self-adaptive fuzzy PID controller is proposed by Khodayari and Balochian (2015) based on nonlinear MIMO structure for an AUV. A

*Corresponding author, Ph.D., Professor, E-mail: jc343965@gmail.com
[a] Ph.D., E-mail: timchen@tdtu.edu.vn

http://www.techno-press.org/?journal=acd&subpage=7 ISSN: 2383-8477 (Print), 2466-0523 (Online)

dynamic model for an AUV is designed and a virtual prototype is constructed which can be used to test different control method by Liu and Wei 2014, Liu *et al*. 2012, Liu *et al*. 2015. An adaptive control scheme is used to operate AUVs by Yuh (2018). In the presence of uncertainties and changing environment conditions, the designed controller performed well even. In adaptive dynamic programming(ADP), the policy and value iteration algorithms are usually used to solve the HJB equation indirectly. So the algorithms have got more and more attention in recent years. The data-driven optimal algorithm is proposed which used the policy iterative algorithm to control temperature of water gas shift reaction. Liu *et al*. The value iteration of ADP is realized by globalized DHP (GDHP). Wei *et al*. 2015, Wei *et al*. 2016 considered The optimal multi-battery coordination control scheme is considered which used a distributed value iterative algorithm to manage the home energy. The policy iteration algorithm is used to solve a class of nonlinear zero-sum differential games. The online actor-critic identifier architecture is proposed to make use of policy iteration algorithms in order to approximate the optimal control law for uncertain nonlinear systems. The policy learning algorithm is proposed to solve state feedback control of unknown affine nonlinear discrete-time systems. The robust model predictive control algorithm is introduced by Shi and Mao 2017 to solve the convex optimization problems in a con strained nonlinear system with bounded persistent disturbance. The main contributions of this paper include the following. (i) ADP control scheme is proposed to solve the optimal trajectory tracking control problem of AUV. (ii) Two iteration procedures are used in the method, which are the i-iteration and the j-iteration. (iii) The optimal tracking control problem is converted into an optimal regulation problem by system transformation. Then the optimal regulation problem is solved by the policy iteration adaptive dynamic programming algorithm. The neural networks are used to realize the proposed algorithm and the convergence and optimality properties of the proposed algorithm are analyzed. This paper is organized as follows. In Section 2, AUV model and problem formulation are presented. In Section 3, the derivative and analysis of trajectory tracking control based on ADP algorithm are given. In Section 4, NNs implementation of the policy iteration ADP algorithm for AUV is presented. To show the effectiveness of the proposed approach, the simulation example is shown in section 5. Finally, conclusions are made in Section 5.

2. System description

In order to analyze the motion of the AUV, two coordinate systems are defined as in Fig. 1. One is universal coordinate system and another is local coordinate system which was referred as Chen (2020)

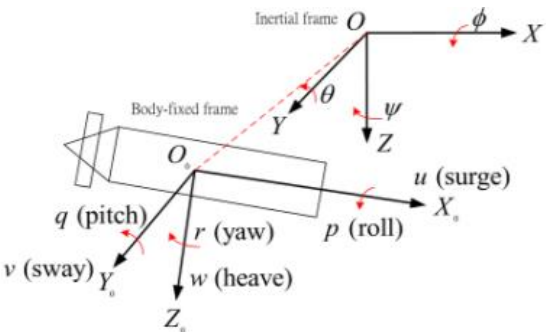

Fig. 1 AUV coordinate systems

x is the location of AUV along the X-direction of universal coordinate system; y is the location of AUV along the Y -direction of universal coordinate system; z is the location of AUV along the Z-direction of universal coordinate system; φ is the roll angle of AUV related to universal coordinate system; θ is the pitch angle of AUV related to universal coordinate system; ψ is the yaw angle of AUV related to universal coordinate system; u is the velocity of AUV along the x direction of local coordinate system; v is the velocity of AUV along the Y -direction of local coordinate system; w is the velocity of AUV along the Z-direction of local coordinate system; p is the roll rate of AUV related to local coordinate system; q is the pitch rate of AUV related to local coordinate system; r is the yaw rate of AUV related to local coordinate system. The dynamic model system is established via laws of Newton. Consider a nonlinear multi-time delay complex system for the approximation of the above AUV described as follows:

$$N_j : \begin{cases} \dot{x}_j(t) = f_j(x_j(t), u_j(t)) + \sum_{k=1}^{G_j} g_{kj}(x_j(t-\tau_{kj})) + \phi_j(t) & (2.1) \\ \phi_j(t) = \sum_{\substack{n=1 \\ n\neq j}}^{J} b_{nj}(x_n(t)), & (2.2) \end{cases}$$

where $f_j(\bullet)$and $g_{kj}(\bullet)$ are the nonlinear vector-valued functions, $x_j(t)$ and $x_j(t-\tau_{kj})$ are the state vector, τ_{kj} denotes the time delay, $u_j(t)$ is the input vector and $b_{nj}(\bullet)$ is the nonlinear interconnection between the *n*th and *j*th subsystems.

The dynamic model is inferred as follows:

$$\begin{aligned} \dot{x}_j(t) &= \frac{\sum_{i=1}^{r_j} w_{ij}(t)[A_{ij}x_j(t) + \sum_{k=1}^{G_j} A_{ikj}x_j(t-\tau_{kj}) + \sum_{\substack{n=1 \\ n\neq j}}^{J} \hat{A}_{inj}x_n(t) + B_{ij}u_j(t)]}{\sum_{i=1}^{r_j} w_{ij}(t)} \\ &= \sum_{i=1}^{r_j} h_{ij}(t)[A_{ij}x_j(t) + \sum_{k=1}^{G_j} A_{ikj}x_j(t-\tau_{kj}) + \sum_{\substack{n=1 \\ n\neq j}}^{J} \hat{A}_{inj}x_n(t) + B_{ij}u_j(t)] \end{aligned} \tag{2.3}$$

In the next section, the PDC scheme is utilized to design the fuzzy controllers.

3. Parallel distributed compensation

According to the decentralized control scheme, the The *j*th fuzzy controller is in the following form:

$$\begin{aligned} &\text{Rule } i\text{: IF } x_{1j}(t) \text{ is } M_{i1j} \text{ and} \cdots \text{and } x_{\eta j}(t) \text{ is } M_{i\eta j} \\ &\text{THEN } u_j(t) = -K_{ij}x_j(t), \end{aligned} \tag{3.1}$$

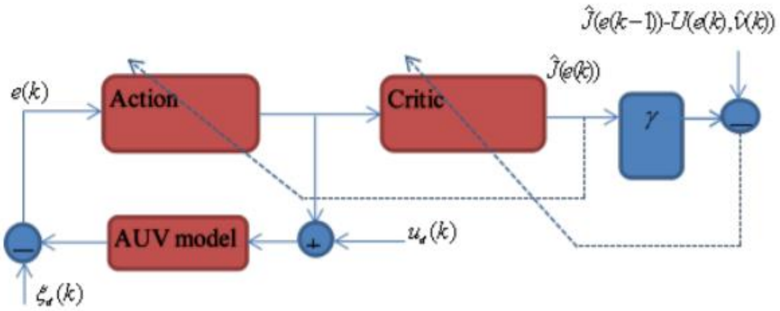

Fig. 2 Structure diagram of ADP controller

where i =1, 2,…, r_j. Hence, the final output of the model based fuzzy controller is

$$u_j(t) = -\frac{\sum_{i=1}^{r_j} w_{ij}(t) K_{ij} x_j(t)}{\sum_{i=1}^{r_j} w_{ij}(t)} = -\sum_{i=1}^{r_j} h_{ij}(t) K_{ij} x_j(t). \tag{3.2}$$

NN is used to approximate nonlinear functions as an effective tool. Two NNs are introduced to realize the proposed algorithm and approximate J^ i,ji (e(k)) and υ^i(k). The NNs include critic network and action network. The structure diagram of ADP algorithm based on policy iteration is shown in Fig. 2.

The final output of the NN model can then be inferred to be

$$\dot{X}(t) = \Psi^S(W^S \Psi^{S-1}(W^{S-1}\Psi^{S-2}(\cdots\cdots \Psi^2(W^2\Psi^1(W^1\Lambda(t)))\cdots\cdots))) \tag{3.3}$$

where

$$\Lambda^T(t) = [X^T(t) \quad U^T(t)] \tag{3.4}$$

with

$$X^T(t) = [x_1(t) \quad x_2(t) \quad \cdots \quad x_\delta(t)], \quad U^T(t) = [u_1(t) \quad u_2(t) \quad \cdots \quad u_m(t)] \tag{3.5}$$

An LDI state-space representation is adopted below in order to derive the LMI inequality and deal with the stability problems described in the state-space representation as (Luan *et al.* 2010).

$$\dot{Y}(t) = A(a(t))Y(t), \quad A(a(t)) = \sum_{i=1}^{r} h_i(a(t))\overline{A}_i \tag{3.6}$$

Subsequently, the min-max matrix G_ς^σ can be defined as follows:

$$G_\varsigma^\sigma = diag[g(T(v_\varsigma))], \quad \sigma = 1, 2, \cdots, S; \quad \varsigma = 1, 2, \cdots, R^\sigma. \tag{3.7}$$

Two processes are developed to train the critic network in order to update the weights of the critic network, and they are the forward computation process and the error backward propagation process. The critic network is used to output the estimation value of J^ i,ji (e(k)) and to minimize the following error function. The objective of training the action network is to minimize the output from the critic network J(t). We can obtain

$$\dot{X}(t)=[\sum_{\varsigma^S=1}^{2}h_{\varsigma^S}(t)G_{\varsigma}^{S}(W^S[\cdots[\sum_{\varsigma^2=1}^{2}h_{\varsigma^2}(t)G_{\varsigma}^{2}(W^2[\sum_{\varsigma^1=1}^{2}h_{\varsigma^1}(t)G_{\varsigma}^{1}(W^1\Lambda(t))])]\cdots])] \tag{3.8}$$

$$=\sum_{\varsigma^S=1}^{2}\cdots\sum_{\varsigma^2=1}^{2}\sum_{\varsigma^1=1}^{2}h_{\varsigma^S}(t)\cdots h_{\varsigma^2}(t)h_{\varsigma^1}(t)G_{\varsigma}^{S}W^S\cdots G_{\varsigma}^{2}W^2G_{\varsigma}^{1}W^1\Lambda(t)=\sum_{\Omega^{\sigma}}h_{\Omega^{\sigma}}(t)E_{\Omega^{\sigma}}\Lambda(t) \tag{3.9}$$

Finally, based on Eq. (3.6), the dynamics of the NN model (3.9) can be rewritten as the following LDI state-space representation:

$$\dot{X}(t)=\sum_{i=1}^{r}h_i(t)\overline{E}_i\Lambda(t) \tag{3.10}$$

4. Robustness design of fuzzy control

The closed-loop nonlinear subsystem as follows:

$$\begin{aligned}\dot{x}_j(t)&=\sum_{i=1}^{r_j}\sum_{f=1}^{r_j}h_{ij}(t)h_{fj}(t)[(A_{ij}-B_{ij}K_{fj})x_j(t)+\sum_{k=1}^{G_j}\overline{A}_{ikj}x_j(t-\tau_{kj})+\sum_{\substack{n=1,\\ n\neq j}}^{J}\hat{A}_{inj}x_n(t)]\\&\quad+\overline{f_j}(x_j(t))+\sum_{k=1}^{G_j}g_{kj}(x_j(t-\tau_{kj}))+\phi_j(t)\\&\quad-\sum_{i=1}^{r_j}\sum_{f=1}^{r_j}h_{ij}(t)h_{fj}(t)[(A_{ij}-B_{ij}K_{fj})x_j(t)+\sum_{k=1}^{G_j}\overline{A}_{ikj}x_j(t-\tau_{kj})]-\sum_{i=1}^{r_j}h_{ij}(t)\sum_{\substack{n=1,\\ n\neq j}}^{J}\hat{A}_{inj}x_n(t)\\&=\sum_{i=1}^{r_j}\sum_{f=1}^{r_j}h_{ij}(t)h_{fj}(t)[(A_{ij}-B_{ij}K_{fj})x_j(t)+\sum_{k=1}^{G_j}\overline{A}_{ikj}x_j(t-\tau_{kj})+\sum_{\substack{n=1\\ n\neq j}}^{J}\hat{A}_{inj}x_n(t)]\\&\quad+e_j(t)+\sum_{k=1}^{G_j}\overline{e}_j(t-\tau_{kj})+\sum_{\substack{n=1\\ n\neq j}}^{J}\hat{e}_{nj}(t)\end{aligned} \tag{4.1}$$

where $\overline{f_j}(x_j(t))\equiv f_j(x_j(t),u_j(t))$ with $u_j(t)=-\sum_{i=1}^{r_j}h_{ij}(t)K_{ij}x_j(t)$,

$$e_j(t)=\overline{f_j}(x_j(t))-\sum_{i=1}^{r_j}\sum_{f=1}^{r_j}h_{ij}(t)h_{fj}(t)(A_{ij}-B_{ij}K_{fj})x_j(t), \tag{4.2}$$

$$\bar{e}_j(t-\tau_{kj}) = g_{kj}(x_j(t-\tau_{kj})) - \sum_{i=1}^{r_j} h_{ij}(t)\bar{A}_{ikj}x_j(t-\tau_{kj}), \tag{4.3}$$

and

$$\hat{e}_{nj}(t) = b_{nj}(x_n(t)) - \sum_{i=1}^{r_j} h_{ij}(t)\hat{A}_{inj}x_n(t), \tag{4.4}$$

and $\Delta\Phi_j \equiv e_j(t) + \sum_{k=1}^{G_j}\bar{e}_j(t-\tau_{kj}) + \sum_{\substack{n=1,\\ n\neq j}}^{J}\hat{e}_{nj}(t)$ denotes the modeling error by the following assumptions.

$$\| e_j(t) \| \le \left\| \sum_{i=1}^{r_j}\sum_{f=1}^{r_j} h_{ij}(t)h_{fj}(t)\Delta H_{ifj}x_j(t) \right\|, \tag{4.5}$$

$$\| \bar{e}_j(t-\tau_{kj}) \| \le \left\| \sum_{i=1}^{r_j} h_{ij}(t)\Delta\bar{H}_{ikj}x_j(t-\tau_{kj}) \right\| \tag{4.6}$$

$$\| \hat{e}_{nj}(t) \| \le \left\| \sum_{i=1}^{r_j} h_{ij}(t)\Delta\hat{H}_{inj}x_n(t) \right\| \tag{4.7}$$

we have

$$e_j^T(t)e_j(t) \le \{\sum_{i=1}^{r_j}\sum_{f=1}^{r_j} h_{ij}(t)h_{fj}(t)\Delta H_{ifj}x_j(t)\}^T\{\sum_{i=1}^{r_j}\sum_{f=1}^{r_j} h_{ij}(t)h_{fj}(t)\Delta H_{ifj}x_j(t)\} \tag{4.8}$$

$$= \{\sum_{i=1}^{r_j}\sum_{f=1}^{r_j} h_{ij}(t)h_{fj}(t)\delta_{ifj}H_{qj}x_j(t)\}^T\{\sum_{i=1}^{r_j}\sum_{f=1}^{r_j} h_{ij}(t)h_{fj}(t)\delta_{ifj}H_{qj}x_j(t)\} \tag{4.9}$$

$$= x_j^T(t)H_{qj}^T[\sum_{i=1}^{r_j}\sum_{f=1}^{r_j} h_{ij}(t)h_{fj}(t)\delta_{ifj}^T][\sum_{i=1}^{r_j}\sum_{f=1}^{r_j} h_{ij}(t)h_{fj}(t)\delta_{ifj}]H_{qj}x_j(t) \tag{4.10}$$

$$\begin{aligned} &\le \left\|\sum_{i=1}^{r_j}\sum_{f=1}^{r_j} h_{ij}(t)h_{fj}(t)\delta_{ifj}^T\right\|\left\|\sum_{i=1}^{r_j}\sum_{f=1}^{r_j} h_{ij}(t)h_{fj}(t)\delta_{ifj}\right\|[H_{qj}x_j(t)]^T[H_{qj}x_j(t)] \\ &\le [H_{qj}x_j(t)]^T[H_{qj}x_j(t)]. \end{aligned} \tag{4.11}$$

In similar fashion, we have

$$\bar{e}_j^T(t-\tau_{kj})\bar{e}_j(t-\tau_{kj}) \le [\bar{H}_{qj}x_j(t-\tau_{kj})]^T[\bar{H}_{qj}x_j(t-\tau_{kj})] \tag{4.12}$$

$$\hat{e}_{nj}^{T}(t)\hat{e}_{nj}(t) \leq [\hat{H}_{qj}x_{n}(t)]^{T}[\hat{H}_{qj}x_{n}(t)] \tag{4.13}$$

The purpose of this paper is two-fold: to stabilize the closed-loop nonlinear system and to attenuate the influence of the external disturbance on the state variable. According to (Yanık *et al.*2018; Muhammed *et al.* 2018; Kim *et al.* 2018), the disturbance attenuation problem, which is characterized by means of the so-called L_2 gain of a nonlinear system, is defined as follows: Given a real number $\gamma > 0$, it is said that the exogenous input is locally attenuated by γ if there exists a neighborhood U of $\boldsymbol{x} = 0$ such that for every positive integer N and for which the state trajectory of the closed-loop nonlinear system starting from $\boldsymbol{x}(0) = 0$ remains in U

$$\sum_{j=1}^{J}\int_{0}^{t_f} x_j^T(t)Q_j x_j(t)dt \leq \eta_j^2 \sum_{j=1}^{J}\int_{0}^{t_f} \phi_j^T(t)\phi_j(t)dt$$

where $\boldsymbol{Q}$ is a positive definite weighting matrix. The physical meaning is finding an L_2 gain less than or equal to a prescribed number γ (strictly less than 1).

Theorem 1: The multi-time delay complex system with multi-interconnections is asymptotically stable, if there exist positive constants α_j, κ_j, ρ_j, σ_j and η_j, j=1,2,…, J are chosen to satisfy

$$Q_{ifj} < 0 \qquad \text{for } i = 1, 2, \cdots, r_j \tag{4.14a}$$

$$\Psi_{ikj} < 0 \qquad \text{for } i = 1, 2, \cdots, r_j \tag{4.14b}$$

where

$$Q_{ifj} = (A_{ij} - B_{ij}K_{fj})^T \sum_{k=1}^{G_j}\tau_{kj}P_j + P_j\sum_{k=1}^{G_j}\tau_{kj}(A_{ij} - B_{ij}K_{fj}) + \kappa_j\sum_{k=1}^{G_j}\tau_{kj}^2 H_{qj}^T H_{qj} + \varpi_j + \theta_j \tag{4.15}$$

$$\Psi_{ikj} = \{\alpha_j^{-1}G_j\bar{A}_{ikj}^T P_j P_j \bar{A}_{ikj} + \rho_j G_j \bar{H}_{qj}^T \bar{H}_{qj} - R_{kj}\} \tag{4.16}$$

with

$$\varpi_j = \alpha_j G_j \sum_{k=1}^{G_j}\tau_{kj}^2 I + \eta_j J\sum_{k=1}^{G_j}\tau_{kj}^2 I + G_j\kappa_j^{-1}P_j^2 + \rho_j^{-1}G_j\sum_{k=1}^{G_j}\tau_{kj}^2 P_j^2 + JG_j\sigma_j^{-1}P_j^2 + \sum_{d=1}^{G_j}R_{dj} \tag{41.7}$$

$$\theta_j = \sum_{n=1}^{J}\eta_n^{-1}G_n \max_{\mu}\lambda_M(\hat{A}_{\mu jn}^T P_n^2 \hat{A}_{\mu jn})I + \sum_{m=1}^{G_n}\sum_{n=1}^{J}\sigma_n\tau_{mn}^2\hat{H}_{qn}^T\hat{H}_{qn} \tag{4.18}$$

$$P_j = P_j^T > 0 \tag{4.19}$$

$$R_{kj} = R_{kj}^T > 0 \tag{4.20}$$

Proof: See Appendix.

Evolved Bat Algorithm (EBA) is proposed based on the bat echolocation fuzzy complex system in the natural world. Unlike other swarm intelligence algorithms, the strong point of EBA is that it only has one parameter, which is called the medium, needs to be determined before employing the algorithms to solve problems. Choosing different medium determines different searching step size in the evolutionary process. In this study, we choose the air to be the medium because it is the original existence medium in the natural environment where bats live. The operation of EBA can be summarized in following steps:

Initialization: the artificial agents are spread into the solution space by randomly assigning coordinates to them.

Movement: the artificial agents are moved. A random number is generated and then it is checked whether it is larger than the fixed pulse emission rate. If the result is positive, the artificial agent is moved using the random walk process.

$$x_i^t = x_i^{t-1} + D,$$

where x_i^t indicates the coordinate of the i-th artificial agent at the t-th iteration, x_i^{t-1} represents the coordinate of the i-th artificial agent at the last iteration, and D is the moving distance that the artificial agent goes in this iteration.

$$D = \gamma \cdot \Delta T$$

where γ is a constant corresponding to the medium chosen in the experiment, and $\Delta T \in [-1, 1]$ is a random number. $\gamma = 0.17$ is used in our experiment because the chosen medium is air.

$$x_i^{t_R} = \beta\left(x_{\text{best}} - x_i^t\right), \quad \beta \in [0, 1]$$

where β is a random number; x_{best} indicates the coordinate of the near best solution found so far throughout all artificial agents; and $x_i^{t_R}$ represents the new coordinates of the artificial agent after the operation of the random walk process.

5. Algorithm

The complete design procedure can be summarized in the following algorithm.

Problem: For a given nonlinear multi-time delay complex system with multi-interconnections ***N***, how do we synthesize a set of decentralized fuzzy controllers to stabilize the nonlinear multi-time delay complex system with multi-interconnections ***N*** ?

The problem described above can be solved by the following steps.

Step 1: Select fuzzy plant rules and membership function for each nonlinear subsystem to establish its T-S fuzzy model with multiple time delays.

Step 2: Synthesize a set of decentralized fuzzy controllers by the concept of PDC scheme.

Step 3: Based on Eq. (4.15) and Eq. (4.16), the bounding matrices ΔH_{ifj} (= $\delta_{ifj}H_{qj}$), $\Delta \bar{H}_{ikj}$ (= $\delta_{ikj}\bar{H}_{qj}$), and $\Delta \hat{H}_{inj}$ = ($\delta_{inj}\hat{H}_{qj}$) are chosen to satisfy Eq. (4.5), Eq. (4.6) and Eq. (4.7), respectively.

Step 4: Repeat Step 2-3 to find appropriate evolved controllers and the bounding matrices ΔH_{ifj} (= $\delta_{ifj}H_{qj}$), $\Delta \bar{H}_{ikj}$ (= $\delta_{ikj}\bar{H}_{qj}$) and $\Delta \hat{H}_{inj}$ = ($\delta_{inj}\hat{H}_{qj}$) such that the stability criterion is satisfied.

6. Example

In this section, the simulation example is given to demonstrate the effectiveness of the policy iterative ADP algorithm for the optimal trajectory-tracking control problems (Chen *et al*. 2019). Here, we ignore roll motion. So the general dynamic model of under-actuated AUV is used. According to the kinematic model of AUV, we can get the desired position and orientation of AUV and the actual position and orientation of AUV respectively. How do we synthesize three evolved controllers to stabilize the nonlinear multi-time delay complex system with multi-interconnections ***N*** ?

Step 1: We try to use as few rules as possible described by the following evolved models:

T-S evolved model of subsystem 1:

Subsystem 1:

Rule 1: If $x_{11}(t)$ is M_{111}

$$\text{Then } \dot{x}_1(t) = A_{11}x_1(t) + \sum_{k=1}^{3} A_{k1}x_1(t-\tau_{k1}) + \sum_{\substack{n=1\\ n\neq j}}^{3} \hat{A}_{1n1}x_n(t) + B_{11}u_1(t) \ , \tag{6.1}$$

Rule 2: If $x_{11}(t)$ is M_{211}

$$\text{Then } \dot{x}_1(t) = A_{21}x_1(t) + \sum_{k=1}^{3} A_{2k1}x_1(t-\tau_{k1}) + \sum_{\substack{n=1\\ n\neq j}}^{3} \hat{A}_{2n1}x_n(t) + B_{21}u_1(t) \tag{6.2}$$

where $x_1^T(t)=[x_{11}(t)\ \ x_{21}(t)]$, $\tau_{11} = 0.25$ (sec), $\tau_{21} = 0.5$ (sec), $\tau_{31} = 0.85$ (sec)

$$A_{11}=\begin{bmatrix} -14.5 & -1.42 \\ -4.5 & -5.6 \end{bmatrix},\ A_{21}=\begin{bmatrix} -14.5 & -1.4 \\ -4.5 & -5.5 \end{bmatrix},\ A_{111}=\begin{bmatrix} 0.01 & 0.01 \\ 0.01 & 0.01 \end{bmatrix},\ A_{121}=\begin{bmatrix} 0.01 & 0.02 \\ 0.01 & 0.01 \end{bmatrix},$$

$$A_{131}=\begin{bmatrix} 0.01 & 0.01 \\ 0.014 & 0.01 \end{bmatrix},\ A_{211}=\begin{bmatrix} 0.01 & 0.01 \\ 0.01 & 0.01 \end{bmatrix},\ A_{221}=\begin{bmatrix} 0.01 & 0.03 \\ 0.01 & 0.01 \end{bmatrix},\ A_{231}=\begin{bmatrix} 0.01 & 0.01 \\ 0.013 & 0.01 \end{bmatrix}, \tag{6.3}$$

$$\hat{A}_{121} = \begin{bmatrix} 0.3 & 0.2 \\ 0.1 & 0.4 \end{bmatrix},\ \hat{A}_{131} = \begin{bmatrix} 0.3 & 0.2 \\ 0.1 & 0.4 \end{bmatrix},\ \hat{A}_{221} = \begin{bmatrix} 0.3 & 0.1 \\ 0.1 & 0.3 \end{bmatrix},\ \hat{A}_{231} = \begin{bmatrix} 0.3 & 0.1 \\ 0.1 & 0.3 \end{bmatrix},$$

$$B_{11} = \begin{bmatrix} 1 \\ 4.5 \end{bmatrix},\qquad B_{21} = \begin{bmatrix} 1 \\ 4.5 \end{bmatrix} \tag{6.4}$$

and the membership functions for Rule 1 and Rule 2 are

$$M_{111}(x_{11}(t)) = \frac{1}{[1+0.006\times[2-x_{11}(t)]]^2},\quad M_{211}(x_{11}(t)) = 1 - M_{111}(x_{11}(t)).$$

Subsystem 2:

Rule 1: If $x_{12}(t)$ is M_{112}

$$\text{Then } \dot{x}_2(t) = A_{12}x_2(t) + \sum_{k=1}^{3} A_{1k2}x_2(t-\tau_{k2}) + \sum_{\substack{n=1\\ n\neq j}}^{3} \hat{A}_{1n2}x_n(t) + B_{12}u_2(t),$$

Rule 2: If $x_{12}(t)$ is M_{212}

$$\text{Then } \dot{x}_2(t) = A_{22}x_2(t) + \sum_{k=1}^{3} A_{2k2}x_2(t-\tau_{k2}) + \sum_{\substack{n=1\\ n\neq j}}^{3} \hat{A}_{2n2}x_n(t) + B_{22}u_2(t)$$

where $x_2^T(t)=[x_{12}(t)\ \ x_{22}(t)]$, $\tau_{12} = 0.4$ (sec), $\tau_{22} = 0.55$ (sec), $\tau_{32} = 0.65$ (sec)

$$A_{12}=\begin{bmatrix}-15 & 1.72\\ -5 & 0.7\end{bmatrix},\ A_{22}=\begin{bmatrix}-15 & 1.7\\ -5 & 0.4\end{bmatrix},\ A_{112}=\begin{bmatrix}0.01 & 0.01\\ 0.01 & 0.01\end{bmatrix},\ A_{122}=\begin{bmatrix}0.01 & 0.01\\ 0.01 & 0.01\end{bmatrix},$$

$$A_{132}=\begin{bmatrix}0.01 & 0.025\\ 0.01 & 0.01\end{bmatrix},\ A_{212}=\begin{bmatrix}0.01 & 0.01\\ 0.01 & 0.01\end{bmatrix},\ A_{222}=\begin{bmatrix}0.01 & 0.01\\ 0.01 & 0.01\end{bmatrix},\ A_{232}=\begin{bmatrix}0.01 & 0.035\\ 0.01 & 0.01\end{bmatrix}, \tag{6.5}$$

$$\hat{A}_{112}=\begin{bmatrix}0.3 & 0.2\\ 0.1 & 0.8\end{bmatrix},\ \hat{A}_{132}=\begin{bmatrix}0.3 & 0.2\\ 0.1 & 0.4\end{bmatrix},\ \hat{A}_{212}=\begin{bmatrix}0.3 & 0.1\\ 0.1 & 0.1\end{bmatrix},\ \hat{A}_{232}=\begin{bmatrix}0.3 & 0.1\\ 0.1 & 0.3\end{bmatrix},$$

$$B_{12}=\begin{bmatrix}1\\ 4.5\end{bmatrix},\quad B_{22}=\begin{bmatrix}1\\ 4.5\end{bmatrix}$$

and membership functions for Rule 1 and Rule 2 are

$$M_{112}(x_{12}(t))=\frac{1}{[1+0.25\times[2-x_{12}(t)]]^2},\quad M_{212}(x_{12}(t))=1-M_{112}(x_{12}(t)).$$

Subsystem 3:

Rule 1: If $x_{13}(t)$ is M_{113}

Then $\dot{x}_3(t)=A_{13}x_3(t)+\sum_{k=1}^{3}A_{1k3}x_3(t-\tau_{k3})+\sum_{\substack{n=1\\ n\neq j}}^{3}\hat{A}_{1n3}x_n(t)+B_{13}u_3(t)$,

Rule 2: If $x_{13}(t)$ is M_{213}

Then $\dot{x}_3(t)=A_{23}x_3(t)+\sum_{k=1}^{3}A_{2k3}x_3(t-\tau_{k3})+\sum_{\substack{n=1\\ n\neq j}}^{3}\hat{A}_{2n3}x_n(t)+B_{23}u_3(t)$

where $x_3^T(t)=[x_{13}(t)\ \ x_{23}(t)]$, $\tau_{13}=0.15$ (sec), $\tau_{23}=0.5$ (sec), $\tau_{33}=0.95$ (sec)

$$A_{13}=\begin{bmatrix}-13.5 & -1.34\\ -4 & 1.2\end{bmatrix},\ A_{23}=\begin{bmatrix}-13.5 & -1.3\\ -4 & 0.8\end{bmatrix},\ A_{113}=\begin{bmatrix}0.01 & 0.01\\ 0.025 & 0.01\end{bmatrix},\ A_{123}=\begin{bmatrix}0.01 & 0.01\\ 0.01 & 0.01\end{bmatrix},$$

$$A_{133}=\begin{bmatrix}0.01 & 0.01\\ 0.01 & 0.01\end{bmatrix},\ A_{213}=\begin{bmatrix}0.01 & 0.01\\ 0.015 & 0.01\end{bmatrix},\ A_{223}=\begin{bmatrix}0.01 & 0.01\\ 0.01 & 0.01\end{bmatrix},\ A_{233}=\begin{bmatrix}0.01 & 0.01\\ 0.01 & 0.01\end{bmatrix}, \tag{6.6}$$

$$\hat{A}_{113}=\begin{bmatrix}0.3 & 0.2\\ 0.1 & 0.4\end{bmatrix},\ \hat{A}_{123}=\begin{bmatrix}0.3 & 0.2\\ 0.1 & 0.4\end{bmatrix},\ \hat{A}_{213}=\begin{bmatrix}0.3 & 0.1\\ 0.1 & 0.3\end{bmatrix},\ \hat{A}_{223}=\begin{bmatrix}0.3 & 0.1\\ 0.1 & 0.3\end{bmatrix},$$

$$B_{13}=\begin{bmatrix}1\\ 3.5\end{bmatrix},\quad B_{23}=\begin{bmatrix}1\\ 3.5\end{bmatrix},$$

and membership functions for Rule 1 and Rule 2 are

$$M_{113}(x_{13}(t)) = \frac{1}{[1+0.03\times[2-x_{13}(t)]]^2},\quad M_{213}(x_{13}(t)) = 1 - M_{113}(x_{13}(t)).$$

Step 2: In order to stabilize the multi-time delay nonlinear complex system with multi-interconnections ***N***, three model-based evolved controllers which are designed via the concept of PDC scheme are synthesized as follows.

Evolved controller:

$$\begin{aligned} &\text{If } x_{11}(t) \text{ is } M_{11} \text{ Then } u_1(t) = -K_{11}x_1(t), \\ &\text{If } x_{11}(t) \text{ is } M_{21} \text{ Then } u_1(t) = -K_{21}x_1(t). \end{aligned} \tag{6.7}$$

$$\begin{aligned} &\text{If } x_{12}(t) \text{ is } M_{12} \text{ Then } u_2(t) = -K_{12}x_2(t), \\ &\text{If } x_{12}(t) \text{ is } M_{22} \text{ Then } u_2(t) = -K_{22}x_2(t). \end{aligned} \tag{6.8}$$

$$\begin{aligned} &\text{If } x_{13}(t) \text{ is } M_{13} \text{ Then } u_3(t) = -K_{13}x_3(t), \\ &\text{If } x_{13}(t) \text{ is } M_{23} \text{ Then } u_3(t) = -K_{23}x_3(t). \end{aligned} \tag{6.9}$$

Steps 3-4: In accordance with Remark 1, the bounding matrices are chosen as

$$\begin{aligned}
&H_{q1} = \begin{bmatrix} 1.9 & -0.4 \\ -0.4 & 1.9 \end{bmatrix},\quad H_{q2} = \begin{bmatrix} 0.6 & -0.3 \\ -0.3 & 0.6 \end{bmatrix},\quad H_{q3} = \begin{bmatrix} 1.5 & -0.5 \\ -0.5 & 1.5 \end{bmatrix}, \\
&\delta_{ifj} = I \quad \text{for} \quad i, f = 1, 2;\quad j = 1, 2, 3. \\
&\overline{H}_{q1} = \begin{bmatrix} 1.2 & -0.3 \\ -0.3 & 1.2 \end{bmatrix},\quad \overline{H}_{q2} = \begin{bmatrix} 1.2 & -0.3 \\ -0.3 & 1.2 \end{bmatrix},\quad \overline{H}_{q3} = \begin{bmatrix} 1.2 & -0.3 \\ -0.3 & 1.2 \end{bmatrix}, \\
&\delta_{ikj} = I \quad \text{for} \quad i = 1, 2;\quad k,\ j = 1, 2, 3. \\
&\hat{H}_{q1} = \begin{bmatrix} 0.2 & -0.1 \\ -0.1 & 0.3 \end{bmatrix},\quad \hat{H}_{q2} = \begin{bmatrix} 0.2 & -0.1 \\ -0.1 & 0.3 \end{bmatrix},\quad \hat{H}_{q3} = \begin{bmatrix} 0.2 & -0.1 \\ -0.1 & 0.3 \end{bmatrix}, \\
&\delta_{inj} = I \quad \text{for} \quad i = 1, 2;\quad n,\ j = 1, 2, 3.
\end{aligned} \tag{6.10}$$

Subsequently, for the purpose of fulfilling the stability conditions of Theorem 1, selecting the proper common positive definite matrix P and the control force K becomes the key problem to be dealt with. In this paper, we use EBA to discover the proper solutions. In this case, the obtained solutions can be classified into two categories: feasible and infeasible. It means that designing the fitness function in a binary operation form is a simpler way to answer to the need of this application. In this paper, the fitness function is designed based on the stability criterion derived from the LMI conditions via the Lyapunov function approach. The AND logical operation is employed in the fitness function for examining the solutions to produce the binary classification results on the discovered solutions. The fitness function is formulated as follows:

$$P_1 = \begin{bmatrix} 6.5 & -1.7 \\ -1.7 & 4.2 \end{bmatrix}, \quad P_2 = \begin{bmatrix} 6.5 & -1.5 \\ -1.5 & 4.2 \end{bmatrix}, \quad P_3 = \begin{bmatrix} 6.5 & -1.6 \\ -1.6 & 4.2 \end{bmatrix} \tag{6.11}$$

with $\eta_1 = 1,\ \eta_2 = 1,\ \eta_3 = 1,\ \sigma_1 = 10,\ \sigma_2 = 10,\ \sigma_3 = 10,\ \kappa_1 = 10,\ \kappa_2 = 10,\ \kappa_3 = 10,$ $\alpha_1 = 1, \alpha_2 = 1, \alpha_3 = 1,\ \rho_1 = 6,\ \rho_2 = 6,\ \rho_3 = 6,$

$$\begin{aligned} R_{11} &= \begin{bmatrix} 29.55 & -12.9506 \\ -12.9506 & 27.55 \end{bmatrix}, R_{21} = \begin{bmatrix} 27.55 & -12.9506 \\ -12.9506 & 28.55 \end{bmatrix}, R_{31} = \begin{bmatrix} 28.55 & -12.9506 \\ -12.9506 & 27.55 \end{bmatrix} \\ R_{12} &= \begin{bmatrix} 27.55 & -12.9506 \\ -12.9506 & 29.55 \end{bmatrix}, R_{22} = \begin{bmatrix} 29.55 & -12.9506 \\ -12.9506 & 27.55 \end{bmatrix}, R_{32} = \begin{bmatrix} 27.55 & -12.9506 \\ -12.9506 & 29.55 \end{bmatrix} \\ R_{13} &= \begin{bmatrix} 28.55 & -12.9506 \\ -12.9506 & 27.55 \end{bmatrix}, R_{23} = \begin{bmatrix} 27.55 & -12.9506 \\ -12.9506 & 29.55 \end{bmatrix}, R_{33} = \begin{bmatrix} 28.55 & -12.9506 \\ -12.9506 & 27.55 \end{bmatrix}, \end{aligned} \tag{6.12}$$

and G_j=3, j=1,2,3.

Substituting Eqs. (6.4-6.6, 6.10-6.11) and the feedback gains K_{ij}' s in Eqs. (6.7–6.9) into Eq. (4.15) yields

$$\begin{aligned} Q_{11} &= \begin{bmatrix} -10.9237 & 9.8957 \\ 9.8957 & -104.4236 \end{bmatrix}, Q_{21} = \begin{bmatrix} -14.6565 & 38.6108 \\ 38.6108 & -129.0491 \end{bmatrix}, Q_{121} = \begin{bmatrix} -14.6565 & 38.6748 \\ 38.6748 & -130.2843 \end{bmatrix}, \\ Q_{211} &= \begin{bmatrix} -10.9237 & 9.8317 \\ 9.8317 & -103.1884 \end{bmatrix}, Q_{12} = \begin{bmatrix} -82.4448 & 54.2689 \\ 54.2689 & -190.1101 \end{bmatrix}, Q_{22} = \begin{bmatrix} -82.4695 & 55.6187 \\ 55.6187 & -190.7171 \end{bmatrix}, \\ Q_{122} &= \begin{bmatrix} -77.0895 & 60.4867 \\ 60.4867 & -181.4011 \end{bmatrix}, Q_{212} = \begin{bmatrix} -77.0648 & 60.1609 \\ 60.1609 & -188.6661 \end{bmatrix}, Q_{13} = \begin{bmatrix} -6.6961 & -20.9149 \\ -20.9149 & -122.8285 \end{bmatrix}, \\ Q_{23} &= \begin{bmatrix} -4.2691 & -2.4059 \\ -2.4059 & -145.6885 \end{bmatrix}, Q_{123} = \begin{bmatrix} -4.2691 & -3.8459 \\ -3.8459 & -140.1077 \end{bmatrix}, Q_{213} = \begin{bmatrix} -6.6961 & -19.4749 \\ -19.4749 & -128.4093 \end{bmatrix}. \end{aligned} \tag{6.13}$$

The inequality (4.15) is satisfied. Therefore, based on the conditions of Theorem 1, the evolved controllers (6.7) –(6.9) can asymptotically stabilize the nonlinear multi-time delay complex system with multi-interconnections $\boldsymbol{N}$. Simulation results of each subsystem are illustrated in Figs. (6.1–6.3) with initial conditions, $x_{11}(0)= -1.2$, $x_{21}(0)= 1.2$, $x_{12}(0)= -1.7$, $x_{22}(0)= 1.85$, $x_{13}(0)= -1.6$ and $x_{23}(0)= 1.5$.

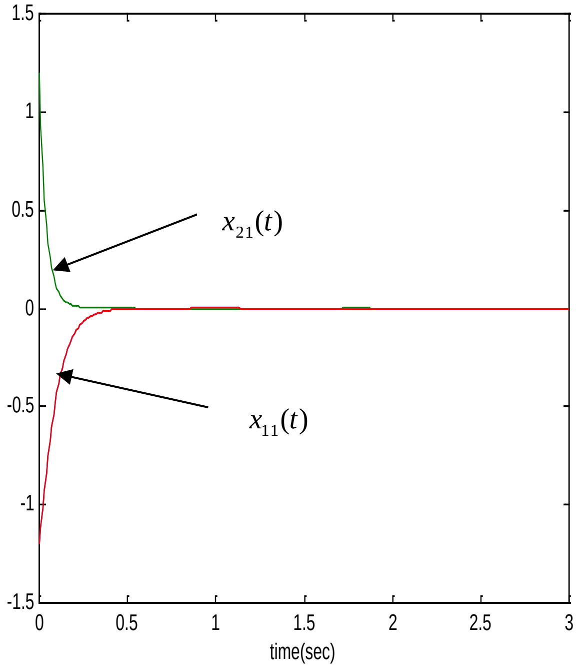

Fig. 6.1 The state response of subsystem 1

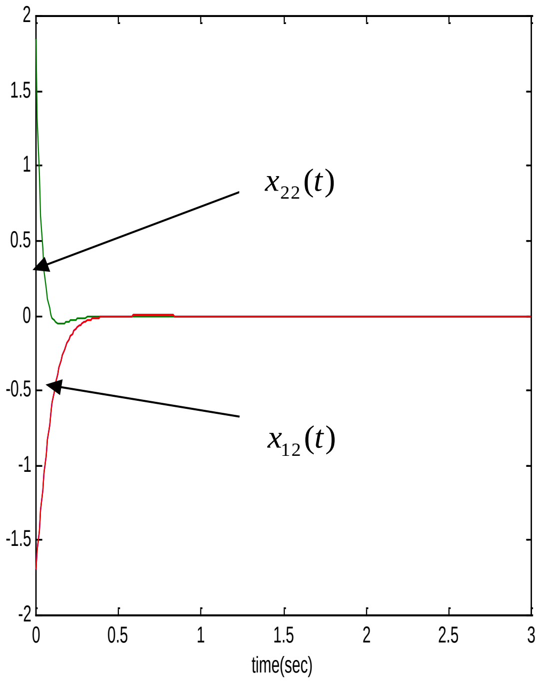

Fig. 6.2 The state response of subsystem 2

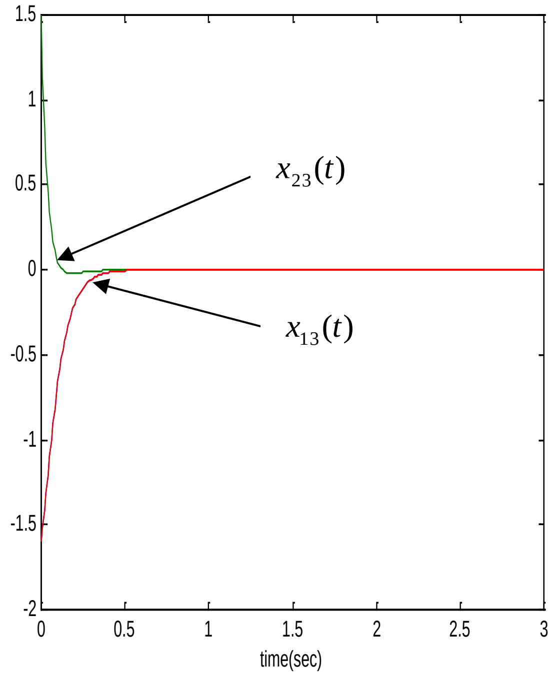

Fig. 6.3 The state response of subsystem 3

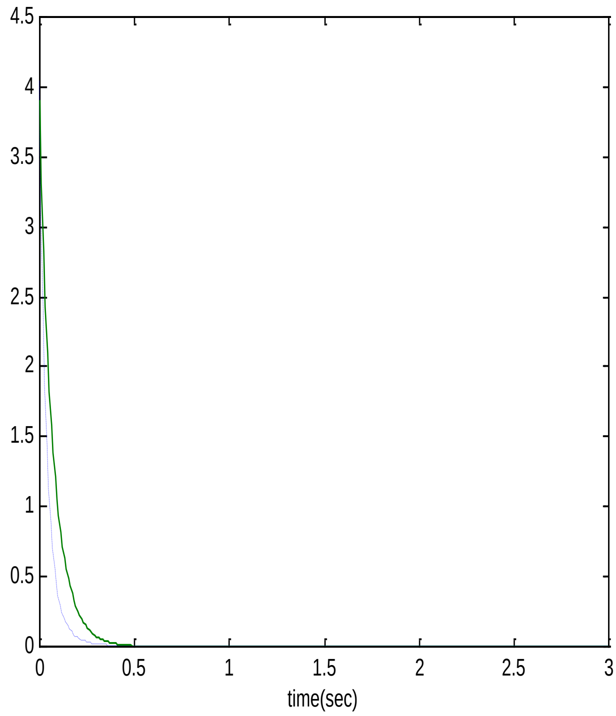

Fig. 6.4 The plots of $\left\|\bar{f}_1(x_1(t)) - \sum_{i=1}^{2}\sum_{f=1}^{2} h_{i1}h_{f1}(t)(A_{i1} - B_{i1}K_{f1})x_1(t)\right\|$ (dashed line) and $\left\|\sum_{i=1}^{2}\sum_{f=1}^{2} h_{i1}h_{f1}(t)\,\Delta H_{if1}x_1(t)\right\|$ (solid line)

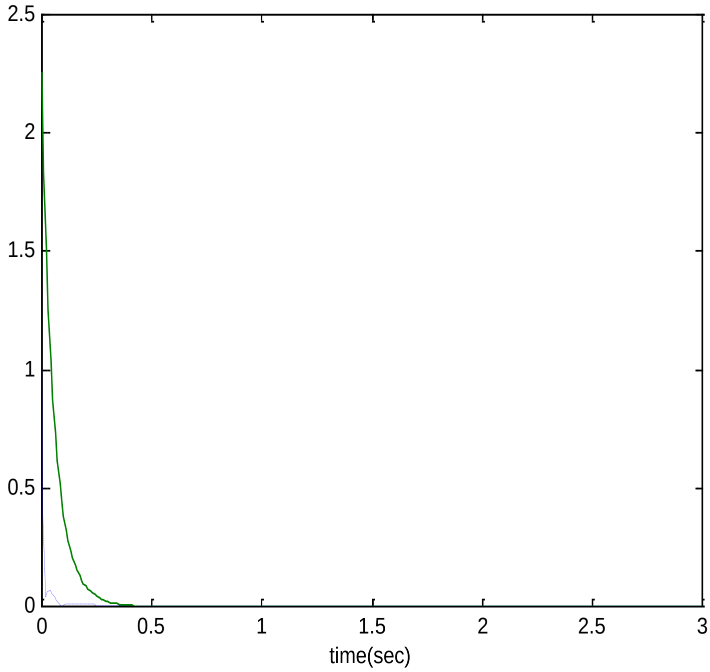

Fig. 6.5 The plots of $\left\|\bar{f}_2(x_2(t)) - \sum_{i=1}^{2}\sum_{f=1}^{2} h_{i2}h_{f2}(t)(A_{i2} - B_{i2}K_{f2})x_2(t)\right\|$ (dashed line) and $\left\|\sum_{i=1}^{2}\sum_{f=1}^{2} h_{i2}h_{f2}(t)\,\Delta H_{if2}x_2(t)\right\|$ (solid line)

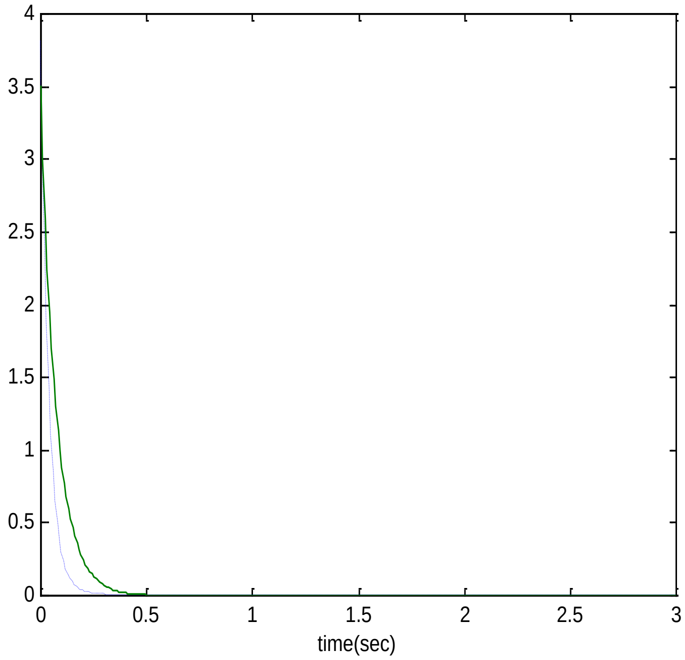

Fig. 6.6 The plots of $\left\|\bar{f}_3(x_3(t)) - \sum_{i=1}^{2}\sum_{f=1}^{2} h_{i3}h_{f3}(t)(A_{i3} - B_{i3}K_{f3})x_3(t)\right\|$ (dashed line) and $\left\|\sum_{i=1}^{2}\sum_{f=1}^{2} h_{i3}h_{f3}(t)\,\Delta H_{if3}x_3(t)\right\|$ (solid line)

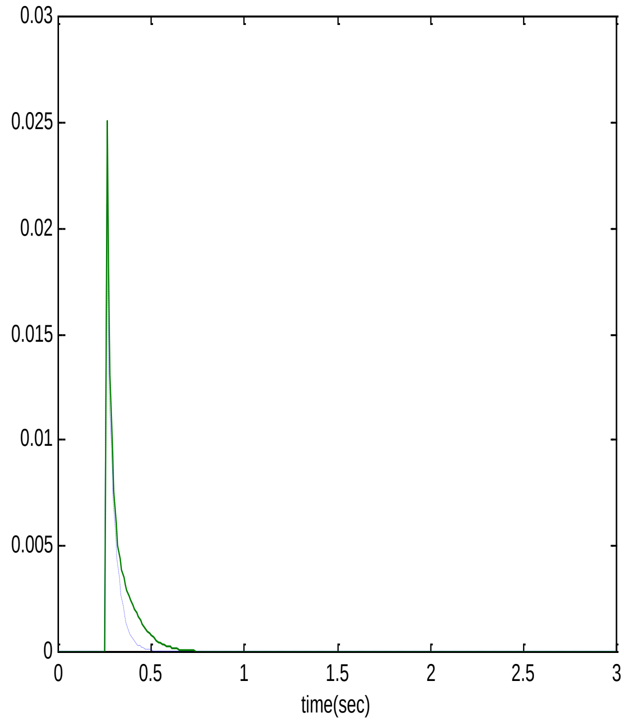

Fig. 6.7 The plots of $\left\|g_{11}\left(x_1(t-0.25)\right)-\sum_{i=1}^{2} h_{i1}(t)(\bar{A}_{i11})\, x_1(t-0.25)\right\|$ (dashed line) and $\|\sum_{i=1}^{2} h_{i1}(t)\Delta\bar{H}_{i11}x_1(t-0.25)\|$(solid line)

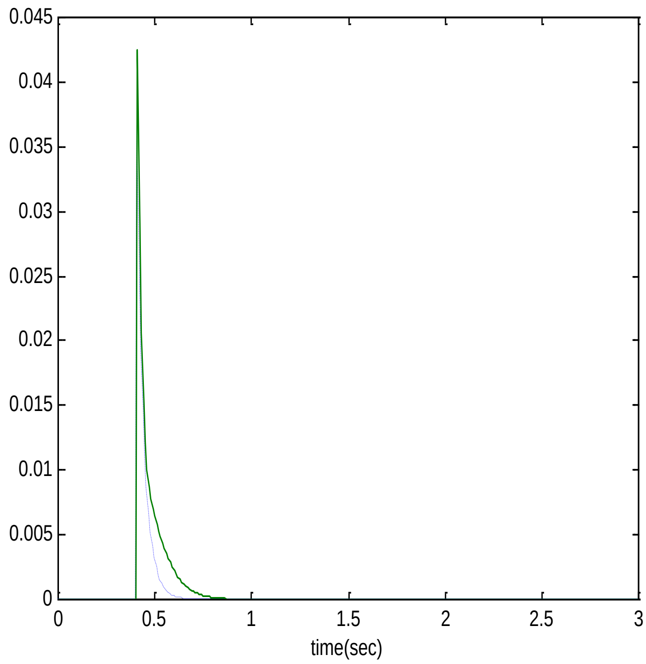

Fig. 6.8 The plots of $\left\|g_{12}\left(x_2(t-0.4)\right)-\sum_{i=1}^{2} h_{i2}(t)(\bar{A}_{i12})\, x_2(t-0.4)\right\|$ (dashed line) and $\|\sum_{i=1}^{2} h_{i2}(t)\Delta\bar{H}_{i12}x_2(t-0.4)\|$ (solid line)

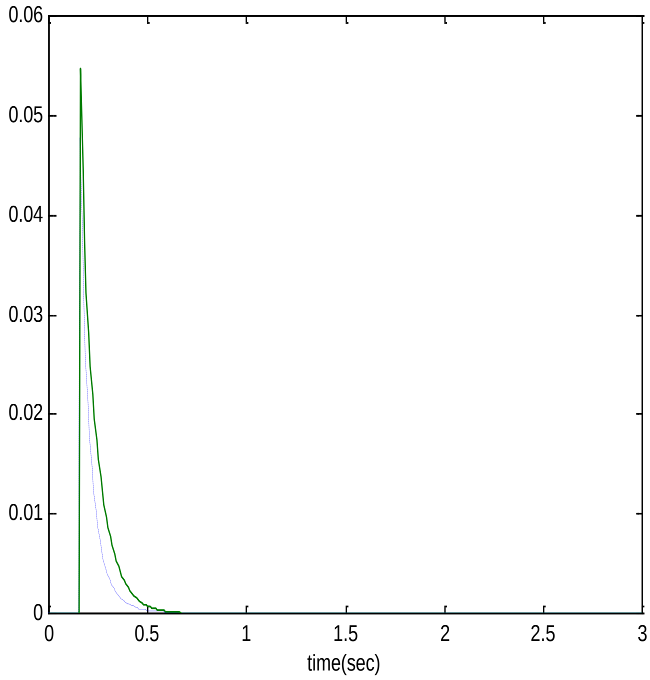

Fig. 6.9 The plots of $\left\|g_{13}\left(x_3(t-0.15)\right)-\sum_{i=1}^{2} h_{i3}(t)(\bar{A}_{i13})\, x_3(t-0.15)\right\|$ (dashed line) and $\|\sum_{i=1}^{2} h_{i3}(t)\Delta\bar{H}_{i13}x_3(t-0.15)\|$ (solid line)

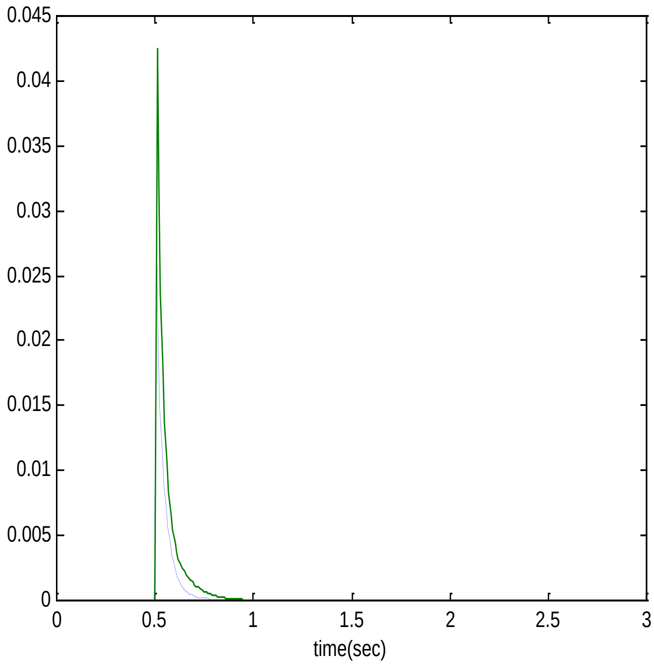

Fig. 6.10 The plots of $\left\|g_{21}\left(x_1(t-0.5)\right)-\sum_{i=1}^{2} h_{i1}(t)(\bar{A}_{i21})\, x_1(t-0.5)\right\|$ (dashed line) and $\|\sum_{i=1}^{2} h_{i1}(t)\Delta\bar{H}_{i21}x_1(t-0.5)\|$ (solid line)

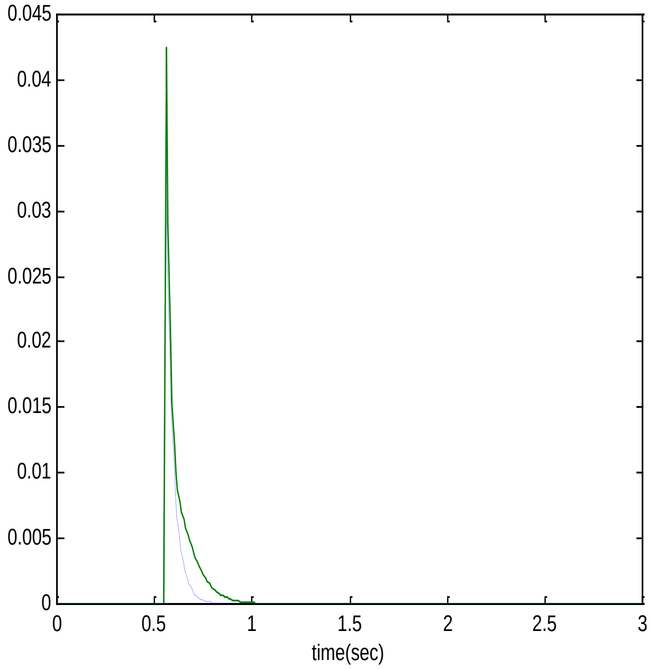

Fig. 6.11 The plots of $\left\|g_{22}\left(x_2(t-0.55)\right)-\sum_{i=1}^{2} h_{i2}(t)(\bar{A}_{i22})\, x_2(t-0.55)\right\|$ (dashed line) and $\|\sum_{i=1}^{2} h_{i2}(t)\Delta\bar{H}_{i22}x_2(t-0.55)\|$ (solid line)

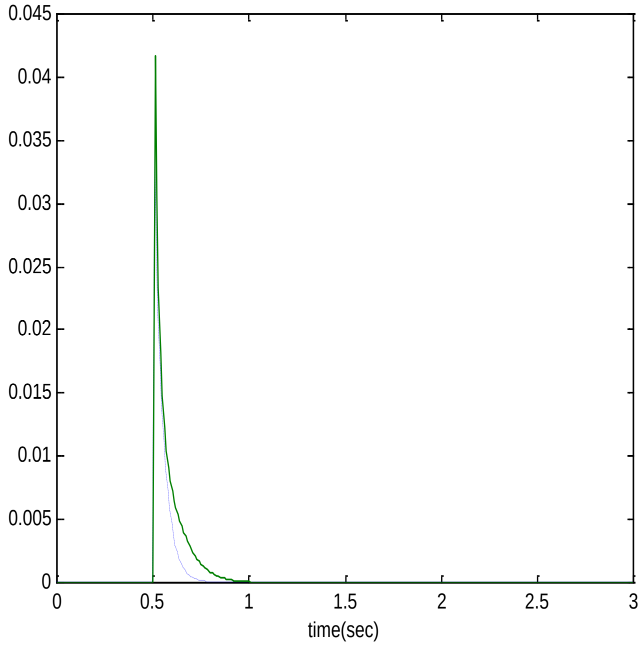

Fig. 6.12 The plots of $\left\|g_{23}\left(x_3(t-0.5)\right)-\sum_{i=1}^{2} h_{i3}(t)(\bar{A}_{i23})\, x_3(t-0.5)\right\|$ (dashed line) and $\|\sum_{i=1}^{2} h_{i3}(t)\Delta\bar{H}_{i23}x_3(t-0.5)\|$ (solid line)

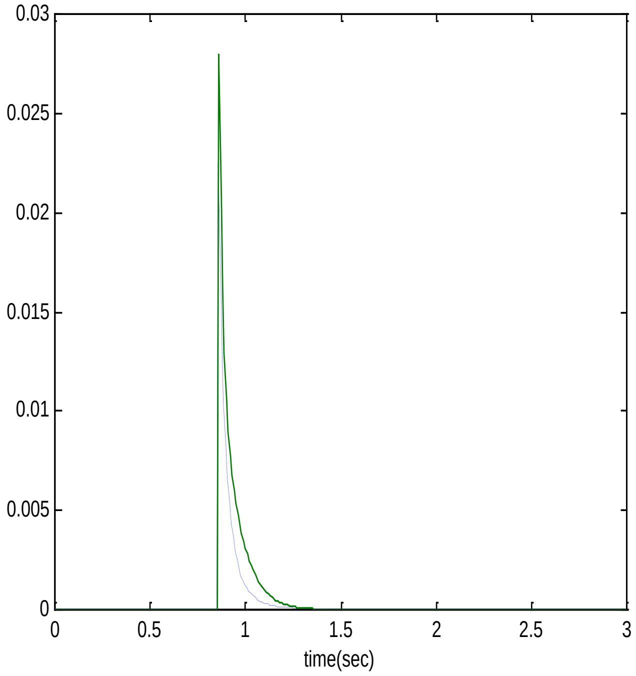

Fig. 6.13 The plots of $\left\|g_{31}\left(x_1(t-0.85)\right)-\sum_{i=1}^{2} h_{i1}(t)(\bar{A}_{i31})\, x_1(t-0.85)\right\|$ (dashed line) and $\|\sum_{i=1}^{2} h_{i1}(t)\Delta\bar{H}_{i31}x_1(t-0.85)\|$ (solid line)

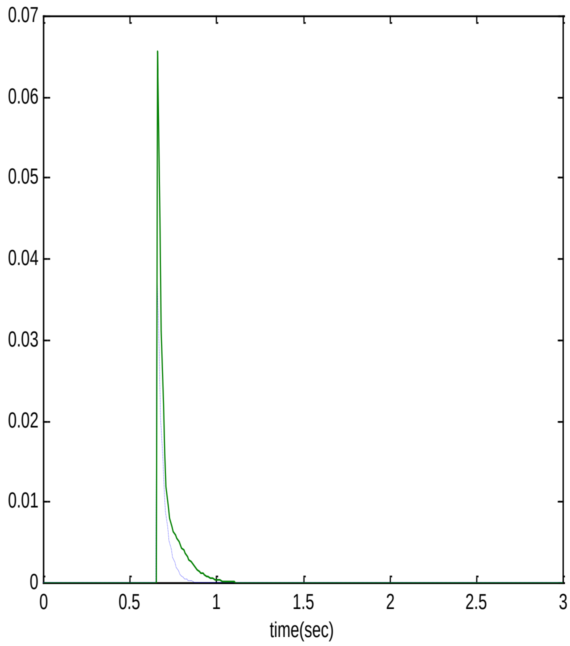

Fig. 6.14 The plots of $\left\|g_{32}\left(x_2(t-0.65)\right)-\sum_{i=1}^{2} h_{i2}(t)(\bar{A}_{i32})\, x_2(t-0.65)\right\|$ (dashed line) and $\|\sum_{i=1}^{2} h_{i2}(t)\Delta\bar{H}_{i32}x_2(t-0.65)\|$ (solid line)

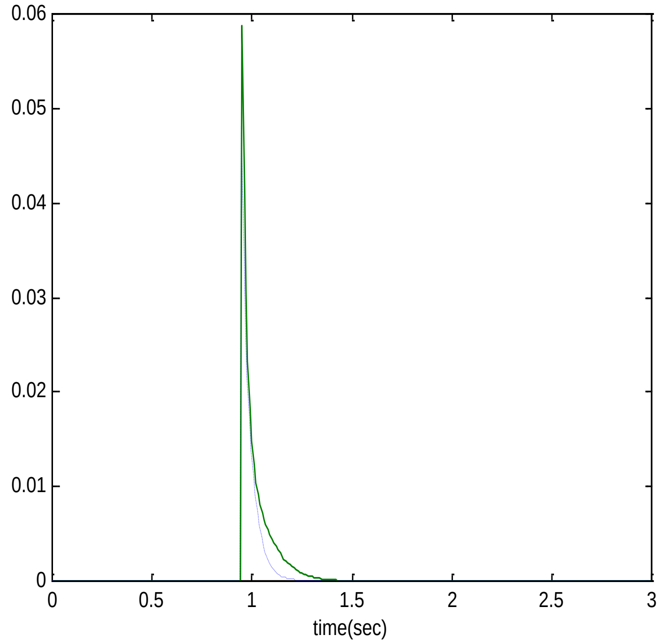

Fig. 6.15 The plots of $\left\| g_{33}\left(x_3(t-0.95)\right) - \sum_{i=1}^{2} h_{i3}(t)(\bar{A}_{i33})\, x_3(t-0.95) \right\|$ (dashed line) and $\| \sum_{i=1}^{2} h_{i3}(t) \Delta \bar{H}_{i33} x_3(t-0.95) \|$ (solid line)

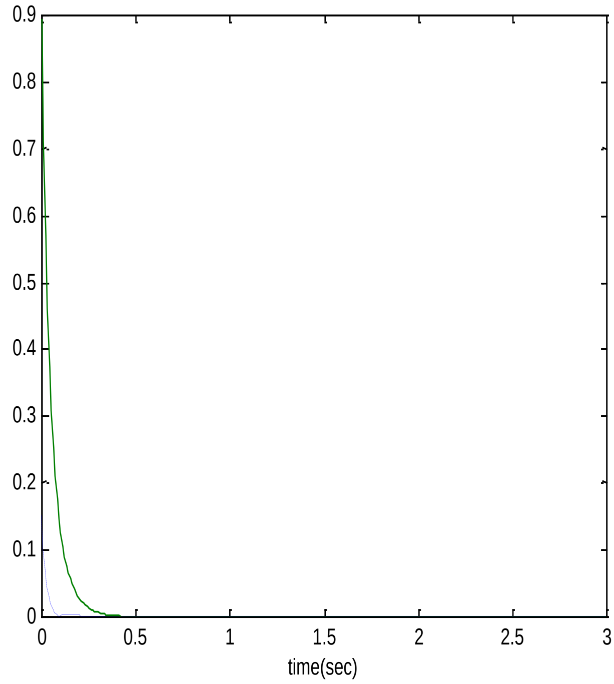

Fig. 6.16 The plots of $\left\| \hat{b}_{21}\left(x_2(t)\right) - \sum_{i=1}^{2} h_{i1}(t) \hat{A}_{i21} x_2(t) \right\|$ (dashed line) and $\left\| \sum_{i=1}^{2} h_{i1}(t) \Delta \widehat{H}_{i21}\, x_2(t) \right\|$ (solid line)

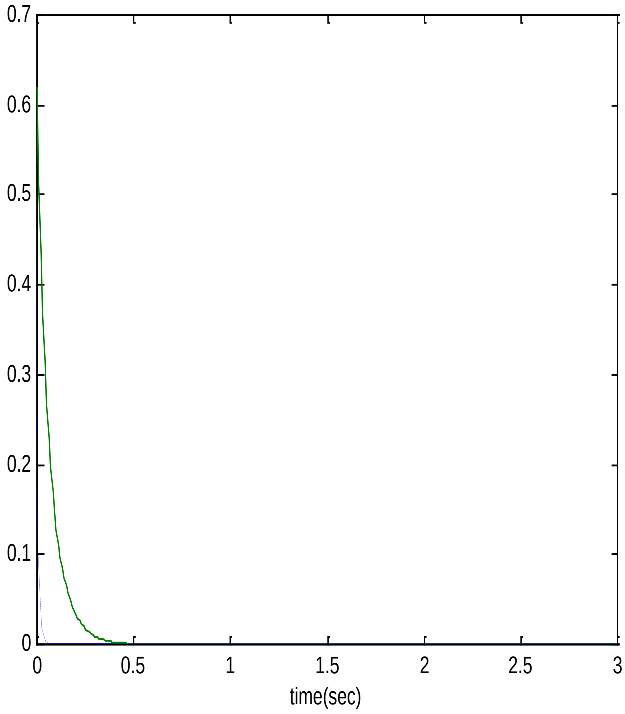

Fig. 6.17 The plots of $\left\|\hat{b}_{31}(x_3(t)) - \sum_{i=1}^{2} h_{i1}(t)\hat{A}_{i31}x_3(t)\right\|$ (dashed line) and $\left\|\sum_{i=1}^{2} h_{i1}(t)\Delta\hat{H}_{i31}\, x_3(t)\right\|$ (solid line)

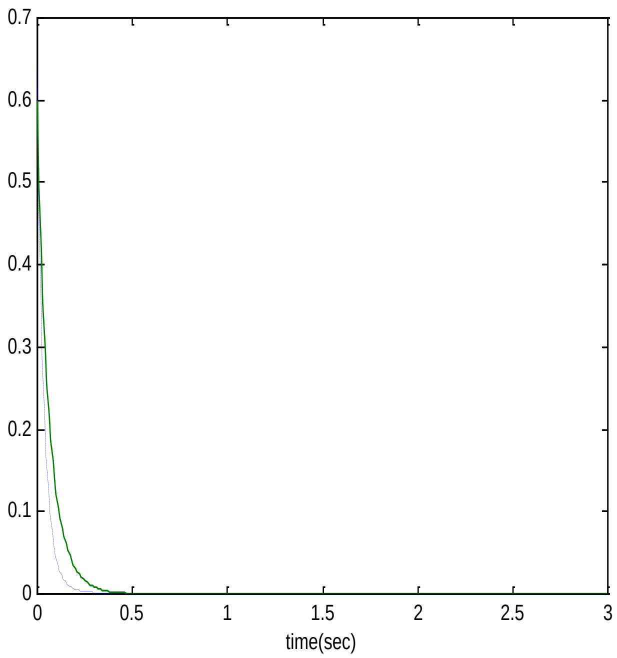

Fig. 6.18 The plots of $\left\|\hat{b}_{12}(x_1(t)) - \sum_{i=1}^{2} h_{i2}(t)\hat{A}_{i12}x_1(t)\right\|$ (dashed line) and $\left\|\sum_{i=1}^{2} h_{i2}(t)\Delta\hat{H}_{i12}\, x_1(t)\right\|$ (solid line)

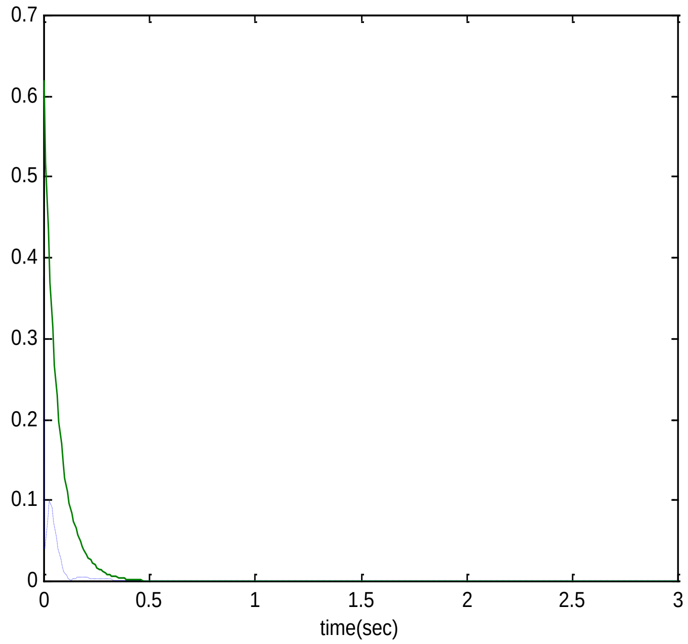

Fig. 6.19 The plots of $\left\|\hat{b}_{32}\big(x_3(t)\big)-\sum_{i=1}^{2}h_{i2}(t)\hat{A}_{i32}x_3(t)\right\|$ (dashed line) and $\left\|\sum_{i=1}^{2}h_{i2}(t)\Delta\hat{H}_{i32}\,x_3(t)\right\|$ (solid line)

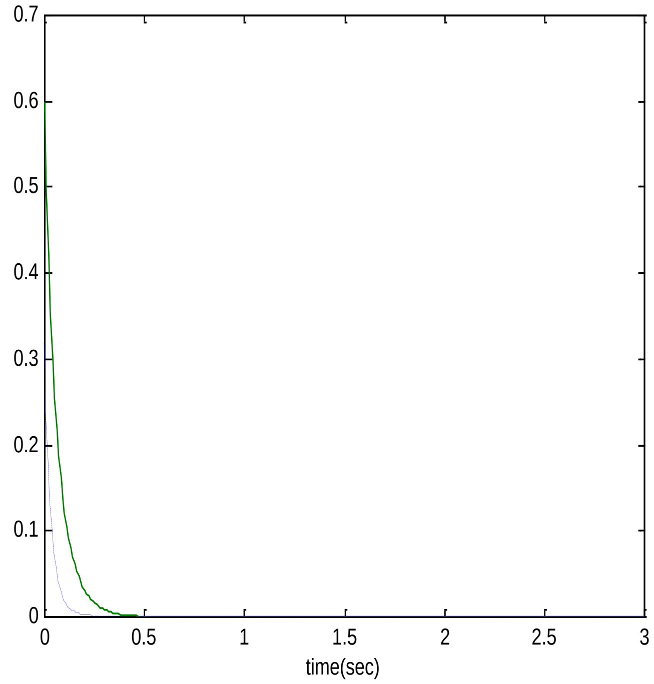

Fig. 6.20 The plots of $\left\|\hat{b}_{13}\big(x_1(t)\big)-\sum_{i=1}^{2}h_{i3}(t)\hat{A}_{i13}x_1(t)\right\|$ (dashed line) and $\left\|\sum_{i=1}^{2}h_{i3}(t)\Delta\hat{H}_{i13}\,x_1(t)\right\|$ (solid line)

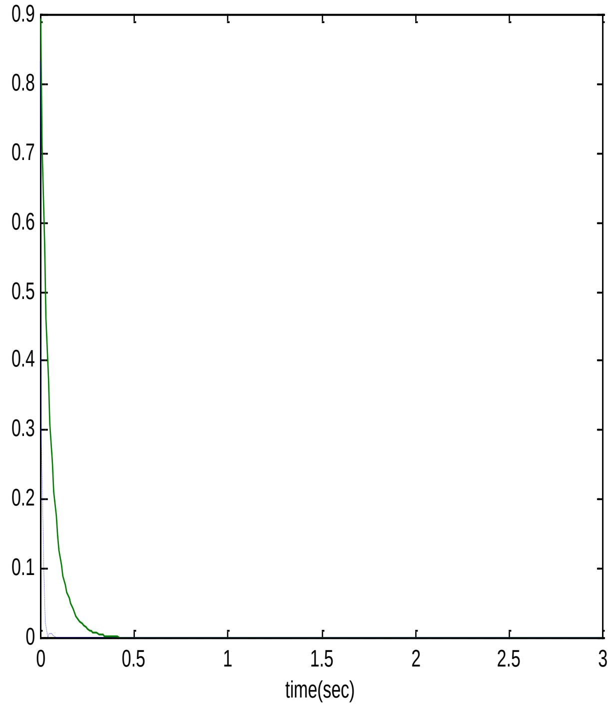

Fig. 6. 21 The plots of $\left\|\hat{b}_{23}\left(x_2(t)\right)-\sum_{i=1}^{2} h_{i3}(t)\hat{A}_{i23}x_2(t)\right\|$ (dashed line) and $\left\|\sum_{i=1}^{2} h_{i3}(t)\Delta\hat{H}_{i23}\, x_2(t)\right\|$ (solid line)

7. Conclusions

In this paper, an effective policy iteration ADP algorithm which is constructed by NNs is proposed to solve the trajectory-tracking control problem of AUV. And the stability of AUV system is analyzed by the proposed control method. According to this criterion and the decentralized control scheme, a set of model-based evolved controllers is synthesized to demonstrate the results.

References

Bedirhanoglu, I. (2014), "A practical neuro-fuzzy model for estimating modulus of elasticity of concrete", *Struct. Eng. Mech*., **51**(2), 249-265. https://doi.org/10.12989/sem.2014.51.2.249

Bhasin, S., Kamalapurkar, R., Johnson, M., Vamvoudakis, K. G., Lewis, F. L. and Dixon, W. E. (2013), "A novel actor-critic-identifier architecture for approximate optimal control of uncertain nonlinear systems", *Automatica*, **49**(1), 82-92. https://doi.org/10.1016/j.automatica.2012.09.019.

Chen, C.W. (2014a), "Interconnected TS fuzzy technique for nonlinear time-delay structural systems", *Nonlinear Dynam*., **76**(1), 13-22.

Chen, C.W. (2014b), "A criterion of robustness intelligent nonlinear control for multiple time-delay systems based on fuzzy Lyapunov methods", *Nonlinear Dynam*., **76**(1), 23-31.

Chen, T., Khurram, S. and Cheng, C. (2019), "A relaxed structural mechanics and fuzzy control for fluid–

structure dynamic analysis", *Eng. Comput*., **36**(7), 2200-2219.

Chen, T., Khurram, S. and Cheng, C. (2019), "Prediction and control of buildings with sensor actuators of fuzzy EB algorithm", *Earthq. Struct.*, **17**(3), 307-315. https://doi.org/10.12989/eas.2019.17.3.307.

Chen, T. (2020), "LMI based criterion for reinforced concrete frame structures", *Adv. Concr. Constr*., 9(4), 407-412.

Chen, T. (2020), "Evolved fuzzy NN control for discrete-time nonlinear systems", *J. Circuits Syst. Comput*., **29**(1), 2050015.

Chen, T. (2020), "On the algorithmic stability of optimal control with derivative operators", *Circuits Syst. Signal Process*., doi:10.1007/s00034-020- 01447-1.

Chen, T. (2020), "An intelligent algorithm optimum for building design of fuzzy structures", *Iran J. Sci. Technol, Trans Civ. Eng*., **44**, 523-531. Khodayari, M. H. and Balochian, S. (2015), "Modeling and control of autonomous underwater vehicle (AUV) in heading and depth attitude via self-adaptive fuzzy PID controller", *J. Marine Sci. Technol*., **20**(3), 559-578. https://doi.org/10.1007/s00773-015-0312-7.

Lin, Q., Wei, Q. and Liu, D. (2017), "A novel optimal tracking control scheme for a class of discrete-time nonlinear systems using generalised policy iterative adaptive dynamic programming algorithm", *Int. J. Syst. Sci*., **48**(3), 525-534. https://doi.org/10.1080/00207721.2016.1188177.

Liu, D. and Wei, Q. (2014), "Data-driven neuro-optimal temperature control of water gas shift reaction using stable iterative adaptive dynamic programming", *IEEE Trans. Ind. Electron*., **61**(11), 6399-6408. https://doi.org/10.1109/TIE.2014.2301770.

Liu, D.,Wang, D.,Zhao, D.,Wei, Q. and Jin, N. (2012), "Neuralnetwork-based optimal control for a class of unknown discretetime nonlinear systems using globalized dual heuristic programming", IEEE *Trans. Autom. Sci. Eng*., **9**(3), 628- 634. https://doi.org/10.1109/TASE.2012.2198057.

Liu, G., Chen, G., Jiao, J. and Jiang, R. (2015), "Dynamics Modeling and Control Simulation of an Autonomous Underwater Vehicle", *J. Coastal Res*., 741-746. https://doi.org/10.2112/SI73-127.1.

Mansour, K., Wu, H. and Hwang, C. (2017), "Nonlinear trajectorytracking control of an autonomous underwater vehicle", *Ocean Eng*., **145**, 188-198. https://doi.org/10.1016/j.oceaneng.2017.08.025.

Santhakumar, M., Asokan, T. (2013), "Power efficient dynamic station keeping control of a flat-fish type autonomous underwater vehicle through design modifications of thruster configuration", *Ocean Eng*., **58**, 11-21. https://doi.org/10.1016/j.oceaneng.2012.09.017.

Shariatmadar, H. and Razavi, H.M. (2014), "Seismic control response of structures using an ATMD with fuzzy logic controller and PSO method", *Struct. Eng. Mech*., **51**(4), 547-564. https://doi.org/10.12989/sem.2014.51.4.547

Shi, D., Mao, Z. (2017), "Multi-step control set-based nonlinear model predictive control with persistent disturbances", *Asian J. Control*, **21**(3), 1-11. https://doi.org/10.1002/asjc.1786.

Son, L., Bur, M., Rusli, M. and Adriyan, A. (2016), "Design of double dynamic vibration absorbers for reduction of two DOF vibration system", *Struct. Eng. Mech*., **57**(1), 161-178. https://doi.org/10.12989/sem.2016.57.1.161

Trinh, H. and Aldeen, M. (1995), "A comment on decentralized stabilization of large scale interconnected systems with delays", *IEEE Trans*., AC-40, 914-916

Tsai, P.W., Hayat, T., Ahmad, B. and Chen, C.W. (2015), "Structural system simulation and control via NN based fuzzy model", *Struct. Eng. Mech*., **56**(3), 385-407. https://doi.org/10.12989/sem.2015.56.3.385

Wei, Q., Liu, D. and Yang, X. (2015), "Infinite horizon self-learning optimal control of nonaffine discrete-time nonlinear systems", *IEEE Trans. Neural Netw. Learn. Syst*., **26**(4), 866-879. https://doi.org/10.1109/TNNLS.2015.2401334.

Wei, Q., Liu, D., Shi, G. and Liu, Y. (2015), "Multibattery Optimal multi-battery coordination control for home energy management systems via distributed iterative adaptive dynamic programming", *IEEE Trans. Ind. Electron*., **42**(7), 4203-4214. https://doi.org/10.1109/TIE.2014.2388198.

Wei, Q., Song, R. and Yan, P. (2016), "Data-driven zero-sum neurooptimal control for a class of continuous-time unknown nonlinear systems with disturbance using ADP", *IEEE Trans. Neural Netw. Learn. Syst*., **27**(2), 444-458. https://doi.org/10.1109/TNNLS.2015.2464080.

Xiang, X., Lapierre, L. and Jouvencel, B. (2015), "Smooth transition of AUV motion control: From fullyactuated to under actuated configuration”, *Robot. Auton. Syst.*, **67**, 14-22. https://doi.org/10.1016/j.robot.2014.09.024.

Yao, H. and Yang, G. (2016), “Efficient Multivariable Generalized Predictive Control for Autonomous Underwater Vehicle in Vertical Plane”, *Math. Probl. Eng.*, **2016**, 1-9. https://doi.org/10.1155/2016/4650380.

Yuh, J. (1990), “Modeling and control of underwater robotic vehicles”, *IEEE Trans. Syst. Man. Cybern., Syst.,* **20**(6), 1475-1483. https://doi.org/10.1109/21.61218.

Zandi, Y., Shariati, M., Marto, A., Wei, X., Karaca, Z., Dao, D., Toghroli, A., Hashemi, M.H., Sedghi, Y., Wakil, K. and Khorami, M. (2018), “Computational investigation of the comparative analysis of cylindrical barns subjected to earthquake”, *Steel Compos. Struct., Int. J.*, **28**(4), 439-447. http://dx.doi.org/10.12989/scs.2018.28.4.439

Zhang, H., Wei, Q. and Liu, D. (2011), “An iterative adaptive dynamic programming method for solving a class of nonlinear zero-sum differential games”, *Automatica*, **47**(1), 207-214. https://doi.org/10.1016/j.automatica.2010.10.033.

Zhang, Y. (2015), “A fuzzy residual strength based fatigue life prediction method”, *Struct. Eng. Mech.*, **56**(2), 201-221. https://doi.org/10.12989/sem.2015.56.2.201

Zhou, X., Lin, Y. and Gu, M. (2015), “Optimization of multiple tuned mass dampers for large-span roof structures subjected to wind loads”, *Wind Struct.*, **20**(3), 363-388. https://doi.org/10.12989/was.2015.20.3.363

WT

Appendix : Proof of Theorem 1

Let the Lyapunov function for the nonlinear multi-time delay complex system with multi-interconnections be defined as

$$V=\sum_{j=1}^{J}v_j(t)=\sum_{j=1}^{J}\{\sum_{k=1}^{G_j}\tau_{kj}x_j^T(t)P_jx_j(t)+\sum_{k=1}^{G_j}\int_0^{\tau_{kj}}x_j^T(t-\tau)R_{kj}x_j(t-\tau)d\tau\} \quad \text{(A1)}$$

where $P_j=P_j^T>0$. We then evaluate the time derivative of V on the trajectories of Eq. (4.1) to get

$$\begin{aligned}
\dot{V}&=\sum_{j=1}^{J}\dot{v}_j(t)=\sum_{j=1}^{J}\sum_{k=1}^{G_j}[\tau_{kj}(\dot{x}_j^T(t)P_jx_j(t)\\
&\quad+x_j^T(t)P_j\dot{x}_j(t))]+\sum_{j=1}^{J}\sum_{k=1}^{G_j}(x_j^T(t)R_{kj}x_j(t)-x_j^T(t-\tau_{kj})R_{kj}x_j(t-\tau_{kj}))\\
&=\sum_{j=1}^{J}\sum_{k=1}^{G_j}\tau_{kj}\{[\sum_{i=1}^{r_j}\sum_{f=1}^{r_j}h_{ij}(t)h_{fj}(t)((A_{ij}-B_{ij}K_{fj})x_j(t)+\sum_{d=1}^{G_j}\overline{A}_{idj}x_j(t-\tau_{dj})\\
&\quad+\sum_{\substack{n=1,\\n\neq j}}^{J}\hat{A}_{inj}x_n(t))+e_j(t)+\sum_{d=1}^{G_j}\overline{e}_j(t-\tau_{dj})+\sum_{\substack{n=1,\\n\neq j}}^{J}\hat{e}_{nj}(t)]^TP_jx_j(t)\\
&\quad+x_j^T(t)P_j[\sum_{i=1}^{r_j}\sum_{f=1}^{r_j}h_{ij}(t)h_{fj}(t)((A_{ij}-B_{ij}K_{fj})x_j(t)+\sum_{d=1}^{G_j}A_{idj}x_j(t-\tau_{dj})\\
&\quad+\sum_{\substack{n=1,\\n\neq j}}^{J}\hat{A}_{inj}x_n(t))+e_j(t)+\sum_{d=1}^{G_j}\overline{e}_j(t-\tau_{dj})+\sum_{\substack{n=1,\\n\neq j}}^{J}\hat{e}_{nj}(t)]\}\\
&\quad+\sum_{j=1}^{J}\sum_{k=1}^{G_j}(x_j^T(t)R_{kj}x_j(t)-x_j^T(t-\tau_{kj})R_{kj}x_j(t-\tau_{kj}))
\end{aligned} \quad \text{(A2)}$$

$$\begin{aligned}
&=\sum_{j=1}^{J}\sum_{k=1}^{G_j}\sum_{i=1}^{r_j}\sum_{f=1}^{r_j}h_{ij}(t)h_{fj}(t)x_j^T(t)[(A_{ij}-B_{ij}K_{fj})^T\tau_{kj}P_j+P_j\tau_{kj}(A_{ij}-B_{ij}K_{fj})]x_j(t)\\
&\quad+\sum_{j=1}^{J}\sum_{k=1}^{G_j}\sum_{i=1}^{r_j}\sum_{d=1}^{G_j}h_{ij}(t)[x_j^T(t-\tau_{dj})\overline{A}_{idj}^TP_j\tau_{kj}x_j(t)+x_j^T(t)\tau_{kj}P_j\overline{A}_{idj}x_j(t-\tau_{dj})]\\
&\quad+\sum_{j=1}^{J}\sum_{k=1}^{G_j}\sum_{n=1}^{J}\sum_{i=1}^{r_j}h_{ij}(t)\sum_{f=1}^{r_j}h_{fj}(t)[x_n^T(t)\hat{A}_{inj}^T\tau_{kj}P_jx_j(t)+x_j^T(t)P_j\tau_{kj}\hat{A}_{inj}x_n(t)]
\end{aligned} \quad \text{(A3)}$$

$$+\sum_{j=1}^{J}\sum_{k=1}^{G_j} [e_j^T(t)P_j\tau_{kj}x_j(t)+x_j^T(t)\tau_{kj}P_je_j(t)]$$

$$+\sum_{j=1}^{J}\sum_{k=1}^{G_j}\sum_{d=1}^{G_j} [\bar{e}_j^T(t-\tau_{dj})P_j\,\tau_{kj}x_j(t)+x_j^T(t)\tau_{kj}P_j\,\bar{e}_j\,(t-\tau_{dj})]$$

$$+\sum_{j=1}^{J}\sum_{k=1}^{G_j}\sum_{\substack{n=1,\\ n\neq j}}^{J}[\hat{e}_{nj}^T(t)P_j\,\tau_{kj}x_j(t)+x_j^T(t)\tau_{kj}P_j\,\hat{e}_{nj}(t)]$$

$$+\sum_{j=1}^{J}\sum_{d=1}^{G_j}(x_j^T(t)R_{dj}x_j(t)-x_j^T(t-\tau_{dj})R_{dj}x_j(t-\tau_{dj}))$$

$$\leq \sum_{j=1}^{J}\sum_{k=1}^{G_j}\sum_{n=1}^{J}\sum_{\mu=1}^{r_n}h_{\mu n}(t)\sum_{i=1}^{r_j}\sum_{m=1}^{G_n}\sum_{f=1}^{r_j}h_{ij}(t)h_{fj}(t)x_j^T(t)\{\frac{1}{JG_n}[(A_{ij}-B_{ij}K_{fj})^T\tau_{kj}P_j+P_j\tau_{kj}(A_{ij}-B_{ij}K_{fj})$$

$$+\alpha_jG_j\tau_{kj}^2I+\eta_jJ\tau_{kj}^2I+\kappa_j^{-1}P_j^2+\rho_j^{-1}G_j\tau_{kj}^2P_j^2+J\sigma_j^{-1}P_j^2$$

$$+\frac{1}{G_j}\sum_{d=1}^{G_j}\bar{P}_{dj}]+\frac{1}{G_nG_j}\eta_n^{-1}G_n\hat{A}_{\mu jn}^TP_n^2\hat{A}_{\mu jn}\}x_j(t)$$

$$+\sum_{j=1}^{J}\sum_{i=1}^{r_j}\sum_{k=1}^{G_j}h_{ij}(t)[\alpha_j^{-1}G_jx_j^T(t-\tau_{kj})\bar{A}_{ikj}^TP_j\,P_j\,\bar{A}_{ikj}x_j(t-\tau_{kj})]$$

$$+\sum_{j=1}^{J}\sum_{k=1}^{G_j}\sum_{n=1}^{J}\sum_{\mu=1}^{r_n}\sum_{i=1}^{r_j}\sum_{f=1}^{r_j}\sum_{m=1}^{G_n} h_{\mu n}(t)h_{ij}(t)h_{fj}(t)\{\frac{1}{JG_n}\kappa_j[H_{qj}x_j(t)]^T\tau_{kj}^2[H_{qj}x_j(t)]\}$$

$$+\sum_{j=1}^{J}\sum_{k=1}^{G_j}\sum_{i=1}^{r_j}h_{ij}(t)\{\rho_jG_j[\bar{H}_{qj}x_j(t-\tau_{kj})]^T[\bar{H}_{qj}x_j(t-\tau_{kj})]\}$$

$$+\sum_{j=1}^{J}\sum_{k=1}^{G_j}\sum_{i=1}^{r_j}\sum_{f=1}^{r_j}\sum_{n=1}^{J}\sum_{m=1}^{G_n}\sum_{\mu=1}^{r_n}h_{\mu n}(t)h_{ij}(t)h_{fj}(t)\{\frac{1}{G_j}\sigma_n[\hat{H}_{qn}x_j(t)]^T\tau_{mn}^2[\hat{H}_{qn}x_j(t)]\}$$

$$+\sum_{j=1}^{J}\sum_{i=1}^{r_j}h_{ij}(t)\sum_{k=1}^{G_j}[-x_j^T(t-\tau_{kj})R_{kj}x_j(t-\tau_{kj})]$$

$$\leq \sum_{j=1}^{J}\sum_{i=1}^{r_j}\sum_{f=1}^{r_j}h_{ij}(t)h_{fj}(t)x_j^T(t)\{[(A_{ij}-B_{ij}K_{fj})^T\sum_{k=1}^{G_j}\tau_{kj}P_j+P_j\sum_{k=1}^{G_j}\tau_{kj}(A_{ij}-B_{ij}K_{fj})$$

$$+\alpha_jG_j\sum_{k=1}^{G_j}\tau_{kj}^2I+\eta_jJ\sum_{k=1}^{G_j}\tau_{kj}^2I+G_j\kappa_j^{-1}P_j^2+\rho_j^{-1}G_j\sum_{k=1}^{G_j}\tau_{kj}^2P_j^2+JG_j\sigma_j^{-1}P_j^2+\sum_{d=1}^{G_j}R_{dj}]$$

$$+\sum_{n=1}^{J}\eta_n^{-1}G_n\max_{\mu}\lambda_M(\hat{A}_{\mu jn}^TP_n^2\hat{A}_{\mu jn})I+\kappa_j\sum_{k=1}^{G_j}\tau_{kj}^2H_{qj}^TH_{qj}+\sum_{m=1}^{G_n}\sum_{n=1}^{J}\sigma_n\tau_{mn}^2\hat{H}_{qn}^T\hat{H}_{qn}\}x_j(t)$$

$$+\sum_{j=1}^{J}\sum_{i=1}^{r_j}\sum_{k=1}^{G_j} h_{ij}(t) x_j^T(t-\tau_{kj})\{\alpha_j^{-1} G_j \overline{A}_{ikj}^T P_j P_j \overline{A}_{ikj} + \rho_j G_j \overline{H}_{qj}^T \overline{H}_{qj} - R_{kj}\} x_j(t-\tau_{kj})$$

$$=\sum_{j=1}^{J}\sum_{i=1}^{r_j}\sum_{f=1}^{r_j} h_{ij}(t) h_{fj}(t) x_j^T(t)[(A_{ij}-B_{ij}K_{fj})^T \sum_{k=1}^{G_j}\tau_{kj} P_j + P_j \sum_{k=1}^{G_j}\tau_{kj}(A_{ij}-B_{ij}K_{fj})$$

$$+\kappa_j \sum_{k=1}^{G_j}\tau_{kj}^2 H_{qj}^T H_{qj} + \varpi_j + \theta_j] x_j(t)$$

$$+\sum_{j=1}^{J}\sum_{i=1}^{r_j}\sum_{k=1}^{G_j} h_{ij}(t) x_j^T(t-\tau_{kj})\{\alpha_j^{-1} G_j \overline{A}_{ikj}^T P_j P_j \overline{A}_{ikj} + \rho_j G_j \overline{H}_{qj}^T \overline{H}_{qj} - R_{kj}\} x_j(t-\tau_{kj})$$

$$=\sum_{j=1}^{J}\sum_{i=1}^{r_j}\sum_{f=1}^{r_j} h_{ij}(t) h_{fj}(t) x_j^T(t) Q_{ifj} x_j(t) + \sum_{j=1}^{J}\sum_{i=1}^{r_j} h_{ij}(t) \sum_{k=1}^{G_j} x_j^T(t-\tau_{kj}) \Psi_{ikj} x_j(t-\tau_{kj}).$$

Based on the Eq. (4.14a) and Eq. (4.14b), we have $\dot{V} < 0$ and the proof is thereby completed.